Chemistry–A European Journal
Research Article
doi.org/10.1002/chem.202301684
Chemistry Europe
European Chemical Societies Publishing
www.chemeurj.org

Reactivity of $[AuF_3(SIMes)]$: Pathway to Unprecedented Structural Motifs

Marlon Winter,[a] Mathias A. Ellwanger,[a, b] Niklas Limberg,[a] Alberto Pérez-Bitrián,[a] Patrick Voßnacker,[a] Simon Steinhauer,[a] and Sebastian Riedel*[a]

We report on a comprehensive reactivity study starting from $[AuF_3(SIMes)]$ to synthesize different motifs of monomeric gold(III) fluorides. A plethora of different ligands has been introduced in a mono-substitution yielding *trans*-$[AuF_2X(SIMes)]$ including alkynido, cyanido, azido, and a set of perfluoroalkoxido complexes. The latter were better accomplished via use of perfluorinated carbonyl-bearing molecules, which is unprecedented in gold chemistry. In case of the cyanide and azide, triple substitution gave rise to the corresponding $[AuX_3(SIMes)]$ complexes. Comparison of the chemical shift of the carbene carbon atom in the $^{13}C\{^1H\}$ NMR spectrum, the calculated SIMes affinity and the Au–C bond length in the solid state with related literature-known complexes yields a classification of *trans*-influences for a variety of ligands attached to the gold center. Therein, the mixed fluorido perfluoroalkoxido complexes have a similar SIMes affinity to AuF_3 with a very low Gibbs energy of formation when using the perfluoro carbonyl route.

Introduction

The chemistry of fluorido organo gold complexes is only scarcely studied compared to that of the heavier halides.[1] This is due to the rather low Au–F bond energy with respect to that of other E–F bonds (E = B, C, Si, P, among others),[2] resulting in a high reactivity of compounds containing Au–F bonds. However, fluorido organo gold complexes are proposed to be important intermediates in gold-mediated and -catalyzed processes, and understanding their reactivity is of great interest in order to develop more efficient catalysts.[3]

The stabilization of such highly reactive species can be achieved upon coordination of strong σ-donors like *N*-heterocyclic carbenes (NHCs) to the gold center. This was shown by the group of *Sadighi* in 2005 with the synthesis of the first fluorido organo gold(I) complex [AuF(SIPr)] (SIPr = 1,3-bis(2,6-diisopropylphenyl)-4,5-dihydroimidazol-2-ylidene),[4] which was later used for the hydrofluorination of alkynes.[5] In the case of gold(III), a handful isolated fluorido organo gold(III) complexes are known. They are either prepared by X/F exchange (X = Cl, Br, I)[6,7,8–10] or by oxidation with XeF_2[11,12] or Selectfluor®.[13] In 2018, our group developed a synthetic route to the first and only fluorido organo gold(III) complex that contains three fluorido ligands, $[AuF_3(SIMes)]$ (SIMes = 1,3-bis(2,4,6-trimethylphenyl)-4,5-dihydroimidazol-2-ylidene).[14] In this complex, the highly Lewis acidic and reactive AuF_3 moiety is stabilized by the NHC SIMes, which makes it easy to handle in standard organic solvents like dichloromethane. Therefore, $[AuF_3(SIMes)]$ can be used for reactivity studies of monomeric AuF_3, which as neat material is polymeric in the solid state[15] and reacts violently with many organic materials.[1]

The solid state structure of $[AuF_3(SIMes)]$ reveals that the Au–F bond length of the fluorido ligand *trans* to the NHC is about 5 pm longer than those of the fluorido ligands in *cis* position.[14] Subsequent studies on the substitution of the fluorido ligand in *trans* position were performed by our group to selectively introduce a chloride,[16] pentafluoroorthotellurate,[16] and trifluoromethyl[17] group via trimethylsilyl reagents (Scheme 1, left). Interestingly, in the reaction with Me_3SiCF_3, also a second and third substitution can be observed, with their ratios depending on the reaction conditions.[17]

The findings summarized on the left side of Scheme 1 show that the combination of $[AuF_3(SIMes)]$ and trimethylsilyl reagents is a promising route for the introduction of a variety of ligands with different donor atoms to the gold center using the formation of gaseous trimethylsilyl fluoride as a driving force. First, we thought of using Me_3SiCCH for the transfer of an ethynido group, similar to a recent work, in which $Me_3SiCCPh$ was used for the successful substitution of fluorido by alkynido ligands.[18] Gold(III) alkynyls in combination with chelating ligands have found application as luminescent materials.[19–27] Furthermore, alkynyl gold(I) complexes bearing NHC ligands have recently shown potential as anticancer drugs.[28] However, corresponding gold(III) complexes are not known, yet. Another interesting group in gold chemistry are pseudohalides like

[a] M. Winter, Dr. M. A. Ellwanger, N. Limberg, Dr. A. Pérez-Bitrián, P. Voßnacker, Dr. S. Steinhauer, Prof. Dr. S. Riedel
Fachbereich Biologie, Chemie, Pharmazie
Institut für Chemie und Biochemie – Anorganische Chemie
Freie Universität Berlin
Fabeckstr. 34/36, 14195 Berlin (Germany)
E-mail: s.riedel@fu-berlin.de

[b] Dr. M. A. Ellwanger
Inorganic Chemistry Laboratory
Department of Chemistry
University of Oxford
South Parks Road, OX1 3QR Oxford, (UK)

Supporting information for this article is available on the WWW under https://doi.org/10.1002/chem.202301684

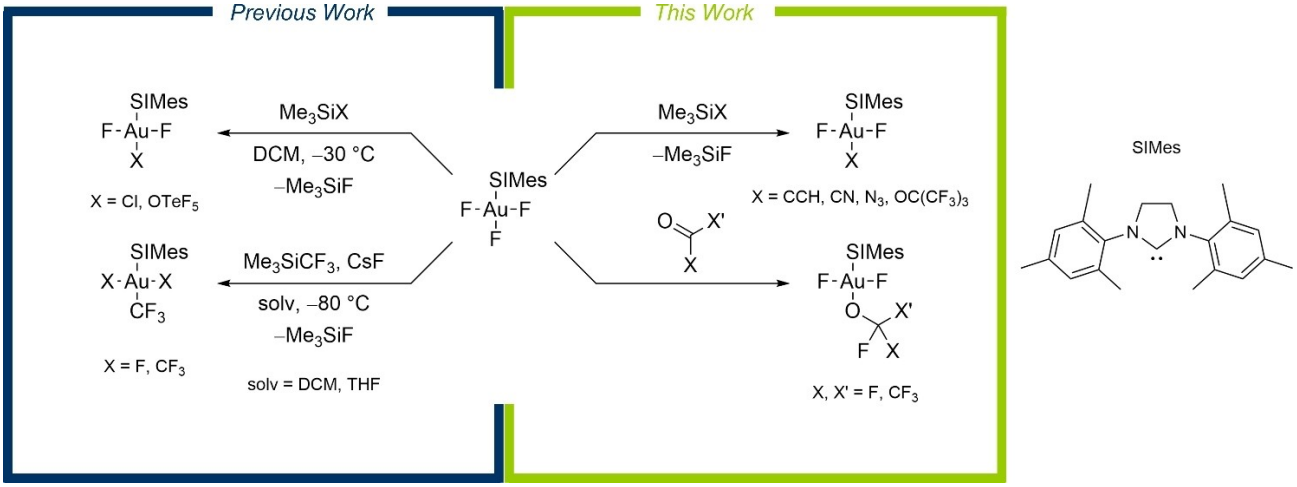

Scheme 1. Overview of the literature-known reactivity of $[AuF_3(SIMes)]$ towards Me_3SiX (X = Cl,[16] $OTeF_5$,[16] CF_3[17]) reagents (left, blue) and the reactivity of $[AuF_3(SIMes)]$ investigated in this work towards trimethylsilyl compounds and perfluorinated carbonyl-bearing molecules (right, green).

cyanide and azide. Cyanide gold chemistry is known for more than a decade.[29] In recent times, cyanido gold(III) complexes with fluorido ligands have been investigated[8,30] including analyses of reductive eliminations from such complexes as C–C bond formation reactions,[9,10] as well as substitution of fluorido by cyanido ligands using Me_3SiCN.[18] A few cyanido gold(I) complexes bearing NHC ligands are known[31,32] but surprisingly, to the best of our knowledge, no such gold(III) complexes are known so far. Azido gold complexes have attracted interest for cycloaddition reactions with alkynes in analogy to the classical copper-catalyzed click chemistry.[33,34] Selected examples of azido gold(I) complexes or compounds formed by their cycloaddition reactions have also been studied for their cytotoxic activity.[34,35] In contrast, for azido gold(III) complexes, only a handful species have been structurally characterized to date.[36–40]

In addition to these C- and N-based functional groups, we turned our attention to the introduction of perfluoroalkoxy groups. Their simplest representative, the trifluoromethoxy group, has distinct electronic[41] and structural[42] properties and metabolic stability. In fact, it has become an important functional group due to the drastic changes it induces in the lipophilicity of an organic compound.[43] In medicinal chemistry, molecules containing an OCF_3 group can be used as drugs for amyotrophic lateral sclerosis (ALS)[44] and work as a SARS-CoV-2 M^{pro} inhibitor.[45] The available methods for the introduction of OCF_3 groups into organic molecules have shown a significant increase in the last two decades, accounting for its importance.[46,47,48,49] However, there is still a lack of general methods and easy-to-handle reagents.[50] In this regard, a significant problem is the equilibrium of the trifluoromethoxide anion with carbonyl fluoride (COF_2) and a fluoride anion,[51–53] which potentially lead to the formation of the corresponding fluorinated molecules as side products, when using salts of the trifluoromethoxide anion.[54] Therefore, some synthetic pathways focus on the in situ preparation of the trifluoromethoxide anion by decomposition of larger molecules.[46,48] There is only one trifluoromethoxido gold complex known, i.e. $[Au(OCF_3)(SIPr)]$, prepared by the reaction of [AuCl(SIPr)] with a solution of $AgOCF_3$ in MeCN.[49] Regarding the higher homologues, i.e. the pentafluoroethoxy and the heptafluoro-*iso*-propoxy groups, the literature-known procedures for their introduction are even scarcer[55] and no gold complexes are known. In contrast, analogous non-fluorinated alkoxido gold complexes are more thoroughly investigated[56] and have been used as a catalyst for Knöevenagel condensation reactions.[57] They can abstract hydrides from metal hydrides yielding gold metal complexes[58] or protons from several organic compounds,[59] as well as cleave C–S[60] and C–Si[61] bonds.

Herein, we present an extensive study of the reactivity of $[AuF_3(SIMes)]$ based on NMR spectroscopy. This includes an expanded investigation of the reaction with trimethylsilyl reagents for the introduction of alkynido, cyanido and azido ligands (see Scheme 1, top right). For the preparation of the first perfluoroalkoxido gold(III) complexes, the route via trimethylsilyl compounds was not possible for the lighter perfluoroalkoxides due to their inherent instability and could only be used for the nonafluoro-*tert*-butoxy group. For the lighter homologues, we exploited the aforementioned equilibrium and directly reacted $[AuF_3(SIMes)]$ with the corresponding perfluorinated carbonyl-bearing molecules (see Scheme 1, bottom right), a route that has also been used for the incorporation of perfluoroalkoxy moieties into phenols,[62] benzyl bromides[53] or metal centers.[51]

Results and Discussion

The ligands that were introduced in the reactivity study can be grouped into three main categories: i) electron donating ligands, i.e. alkynido; ii) pseudohalides, i.e. cyanido and azido; and iii) strongly electron withdrawing ligands, i.e. perfluoroalkoxido.

Introduction of electron-donating ligands

Addition of Me_3SiCCH to a solution of $[AuF_3(SIMes)]$ in dichloromethane (DCM) at −80 °C leads to the desired ethynido complex *trans*-$[Au(CCH)F_2(SIMes)]$ (**1**) (see Scheme 2, top). This compound shows a doublet at −340.8 ppm in the ^{19}F NMR spectrum with a coupling constant of $^4J(^{19}F,^1H) = 2.1$ Hz to the ethynyl proton, which gives the expected triplet in the ^1H NMR spectrum at 1.60 ppm (see Table 1). Additionally, the ^{19}F NMR spectrum shows another signal in the same region, a singlet at −340.2 ppm, which can be assigned to the corresponding trimethylsilyl-substituted alkynido complex *trans*-$[Au(CCSiMe_3)F_2(SIMes)]$ (**2**). Compound **2** could be formed by elimination of HF, a reactivity that has been previously reported for related species.[6,10] In order to verify the formation of compound **2**, the reaction between $[AuF_3(SIMes)]$ and $Me_3SiCCSiMe_3$ was investigated. Monitoring the reaction mixture by multinuclear NMR spectroscopy, the formation of **2** was confirmed (see Table 1 and Scheme 2, bottom). In the $^{13}C\{^1H\}$ NMR spectrum, **1** and **2** also have similar chemical shifts for the carbene carbon atom at 185.3 and 186.4 ppm, respectively, which is particularly sensitive to the nature of the Lewis acidic moiety bound to the Au atom (see below).[16,17,32,63]

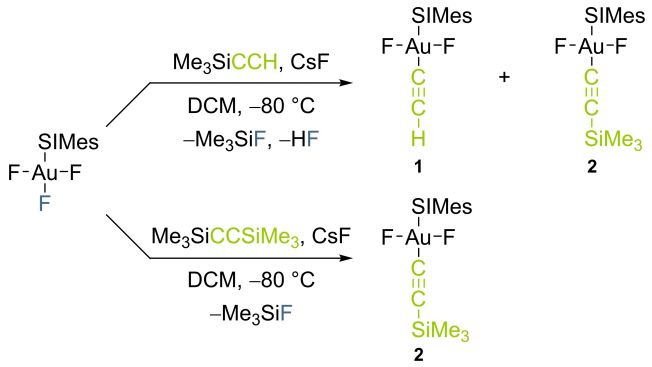

Scheme 2. Reaction of $[AuF_3(SIMes)]$ with different alkynes. Note that the product ratio of the upper reaction depends on the amount of Me_3SiCCH and CsF (see Table S4 and Figure S13).

In order to investigate the conditions that lead to a favored formation of the desired product **1**, the ratio of the reactants and the addition of a fluoride source in the form of CsF was investigated (see Table S4). Without the presence of a fluoride source, *trans*-$[Au(CCH)F_2(SIMes)]$ (**1**) is the main product and only traces of *trans*-$[Au(CCSiMe_3)F_2(SIMes)]$ (**2**) are formed. However, addition of CsF strongly favors the formation of **2** (see Figure S13), as well as the general consumption of $[AuF_3(SIMes)]$.

Single crystals of compound **1** suitable for X-ray diffraction were obtained by vapor diffusion of *n*-pentane onto a concentrated solution of the reaction mixture in DCM at 4 °C. Compound **1** crystallizes in the orthorhombic space group *Pnma* (see Figure 1) and was co-crystallized with about 6% of *trans*-$[AuClF_2(SIMes)]$ (see Figure S1), which itself crystallizes in the same space group with similar lattice parameters.[16] The *trans*-$[AuClF_2(SIMes)]$ is probably formed by Cl/F exchange of unreacted $[AuF_3(SIMes)]$ with DCM, as observed previously when using this solvent.[14] The C≡C bond length of 119.2(8) pm is in the typical range of other gold(III) alkynyl complexes characterized in the solid state.[19–27,64] As expected, the Au–C bond length to the carbene carbon atom (Au–$C_{carbene}$) of 204.8(3) pm is slightly longer than in the literature-known *trans*-$[AuF_2X(SIMes)]$ (X = F,[14] Cl,[16] $OTeF_5$,[16] CF_3[17]) complexes.

Table 1. Selected NMR spectroscopic data of the new compounds described in this article. Chemical shifts δ are given in ppm and coupling constants J in Hz.

Compound[a]	δ_F(Au*F*)[b]	δ_C(NCN)[c]	δ_H(Im-CH_2)[d]	Other NMR signals
$[Au(CCH)F_2(SIMes)]$ (**1**)	−340.8 (d)	185.3	4.17	$\delta_H(CCH) = 1.60$ (t), $^4J(^1H,^{19}F) = 2.1$
$[Au(CCSiMe_3)F_2(SIMes)]$ (**2**)	−340.2	186.4	4.15	$\delta_H(CCSiMe_3) = 0.07$ (s)
$[Au(CN)F_2(SIMes)]$ (**3**)	−337.1	174.6	4.23	–
$[Au(CN)_3(SIMes)]$ (**4**)	–	172.3	4.29	–
$[AuF_2(N_3)(SIMes)]$ (**5**)	−311.1	172.5	4.26	–
$[Au(N_3)_3(SIMes)]$ (**6**)	–	178.1	4.16	–
$[AuF_2(OC(CF_3)_3)(SIMes)]$ (**7**)[e]	−311.9 (dec)	155.7	4.33	$\delta_F((CF_3)_3) = -74.2$ (t), $^5J(^{19}F,^{19}F) = 4.0$
$[AuF_2(OCF_3)(SIMes)]$ (**8**)[e]	−314.1 (q)	152.7	4.35	$\delta_F(CF_3) = -40.2$ (t), $^4J(^{19}F,^{19}F) = 1.9$
$[AuF_2(OC(CF_3)F_2)(SIMes)]$ (**9**)[f]	−314.8	153.6	4.35	$\delta_F(CF_2) = -63.1$ (s); $\delta_F(CF_3) = -86.1$ (s)
$[AuF_2(OC(CF_3)_2F)(SIMes)]$ (**10**)[e]	−313.9 (dsept)	154.5	4.34	$\delta_F((CF_3)_2) = -82.0$ (dt), $^3J(^{19}F,^{19}F) = 3.2$, $^5J(^{19}F,^{19}F) = 1.7$; $\delta_F(CF) = -112.0$ (tsept), $^4J(^{19}F,^{19}F) = 2.4$[g]

[a] The prefix *trans*- was omitted for all *trans*-$[AuF_2X(SIMes)]$ complexes for brevity. [b] δ_F(Au*F*) denotes the chemical shift in the ^{19}F NMR spectrum of the fluorido ligands bound to the gold center. The multiplicity is given in parenthesis in all cases which are not singlets. [c] δ_C(NCN) denotes the chemical shift in the $^{13}C\{^1H\}$ NMR spectrum of the carbene carbon atom. [d] δ_H(Im-CH_2) denotes the chemical shift in the ^1H NMR spectrum of the protons in the backbone of the imidazolidine ring of the NHC. [e] The couplings between the signals in the ^{19}F NMR spectrum were not always observed due to the high linewidth for the signals. Often, the coupling constants were only determinable at high resolution (0.1 Hz). [f] No coupling between the signals in the ^{19}F NMR spectrum was observed due to high linewidth for the signals. However, in the $^{19}F,^{19}F$-COSY NMR spectrum, cross-peaks confirm the assignment to compound **9** (see Figure S41). [g] Coupling constant determined by simulation of the spectrum (see Figure S47).

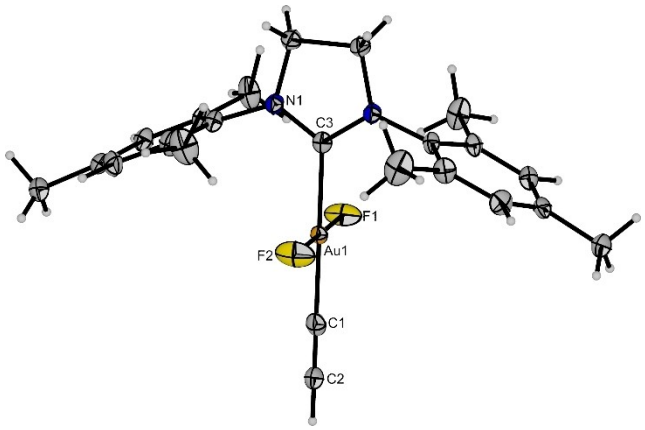

Figure 1. Molecular structure of *trans*-[Au(CCH)F_2(SIMes)] (**1**) in the solid state. The co-crystallization of about 6% of *trans*-[AuClF_2(SIMes)] is omitted for clarity (see Figure S1). Thermal ellipsoids are set at 50% probability. Selected bond lengths [pm]: 198.5(7) (C1–Au1), 204.8(3) (C3–Au1), 193.4(2) (F1–Au1), 193.6(2) (F2–Au1), 119.2(8) (C1–C2).

Introduction of pseudohalides

The introduction of the pseudohalides cyanide and azide to the gold center was performed by the reaction of [AuF_3(SIMes)] with Me_3SiX (X = CN, N_3), as shown in Scheme 3. In both cases, the desired monosubstituted products, *trans*-[Au(CN)F_2(SIMes)] (**3**) and *trans*-[Au$F_2(N_3)$(SIMes)] (**5**), respectively, are formed. However, when more than one equivalent is used, the three times substituted complexes [Au$(CN)_3$(SIMes)] (**4**) and [Au$(N_3)_3$(SIMes)] (**6**) are obtained, respectively.

Interestingly, whereas in case of the cyanide the formation of compound **3** is complete within one day and it fully converts to **4** only after four weeks (see Figure S22), the reaction with the azide is much faster, compound **5** being formed after about one hour and the complete transformation to **6** being achieved within three days (see Figure S29). The only other known reaction of [AuF_3(SIMes)] that led to manifold substitutions of fluorido ligands is the one with Me_3SiCF_3 (see Scheme 1, bottom left).[17] However, in the case of the reaction with Me_3SiCF_3, also the two times substituted product was observed by NMR spectroscopy, contrary to the reaction with Me_3SiX (X = CN, N_3) presented herein, in which none of the *cis*-[AuFX_2(SIMes)] products are observed at any point.

All four compounds **3**–**6** were also analyzed by single-crystal X-ray diffraction. Suitable crystals were obtained in all cases by vapor diffusion of *n*-pentane onto a concentrated solution of the corresponding reaction mixture in DCM at 4 °C. The molecular structure of compound **3**, which crystallizes in the orthorhombic space group *Pnma*, is depicted in Figure 2. The Au–C bond lengths are in the typical range of literature-known cyanido gold(III) complexes.[8,9,12] The structure of compound **4** does not have enough quality to allow structural comparisons, yet it is useful to prove the connectivity and molecular shape of this three times substituted cyanido complex (see Figure S2).

The molecular structures of *trans*-[Au$F_2(N_3)$(SIMes)] (**5**) and [Au$(N_3)_3$(SIMes)] (**6**) are shown in Figure 3. Both compounds crystallize in the triclinic space group $P\bar{1}$. The former crystallizes with half a disordered DCM molecule (see Figure S3) and the latter with a unit cell consisting of two crystallographically independent molecules (see Figure S4). In compound **5**, the azido ligand is oriented parallel to the two fluorido ligands and shows a bent coordination with α(Au–N–N) = 116.9(2)°, which is in-between the average angles for the azido ligands in *cis* (114.2(3)°) and *trans* (119.1(3)°) position to the carbene in compound **6**. The Au–$C_{carbene}$ bond length of 200.9(2) pm in **5** is in the same range as the one in **6** (202.3(4) pm). The Au–N bond lengths in compound **6** do not deviate significantly between the azido ligands *cis* or *trans* to SIMes and lie between 203.1(4) and 204.6(4) pm, which is comparable to the one in **5** (203.5(2) pm), and in the typical range for literature-known gold(III) azido complexes.[36–40]

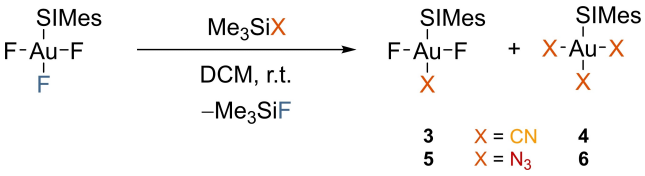

Scheme 3. Reaction of [AuF_3(SIMes)] with Me_3SiX (X = CN, N_3). Note that the ratio of the products depends on the amount of trimethylsilyl reagent that is used. Addition of 1 equivalent of Me_3SiX leads to the monosubstituted products **3** and **5**, while an excess eventually yields the three times substituted complexes **4** and **6** (see Figure S23 and S30, respectively).

Introduction of electron-withdrawing ligands

In order to synthesize the first perfluoroalkoxido gold(III) complex, the reactivity of [AuF_3(SIMes)] towards $Me_3SiOC(CF_3)_3$ was tested. By using this route, *trans*-[Au$F_2(OC(CF_3)_3)$(SIMes)] (**7**) is generated (Scheme 4, top), as detected by ^{19}F NMR spectroscopy. The perfluoro-*tert*-butoxy group gives a triplet at −74.2 ppm, showing a coupling constant of $^5J(^{19}F,^{19}F) = 4.0$ Hz to the decet at −311.9 ppm which belongs to the fluorido ligands attached to the gold center (see Figure 4, left). In the $^{13}C\{^1H\}$ NMR spectrum, the carbene carbon atom of **7** has a

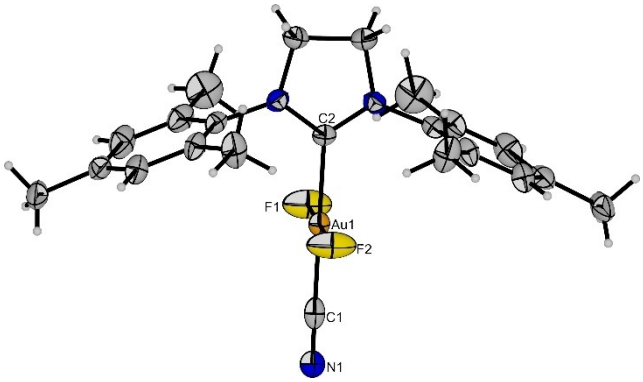

Figure 2. Molecular structure of *trans*-[Au(CN)F_2(SIMes)] (**3**) in the solid state. Thermal ellipsoids are set at 50% probability. Selected bond lengths to the central gold atom [pm]: 202.2(12) (C1–Au1), 202.4(10) (C2–Au1), 191.7(7) (F1–Au1), 193.2(7) (F2–Au1).

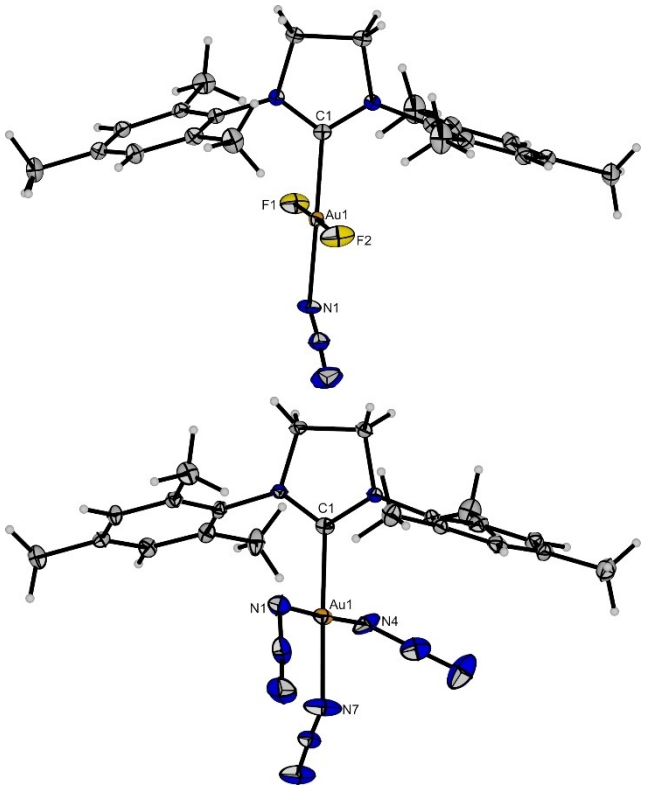

Figure 3. Top: Molecular structure of *trans*-[$AuF_2(N_3)$(SIMes)]·0.5 CH_2Cl_2 (**5**·0.5 CH_2Cl_2) in the solid state. The solvent molecule is omitted for clarity (see Figure S3). Thermal ellipsoids are set at 50% probability. Selected bond lengths to the central gold atom [pm]: 200.9(2) (C1–Au1), 193.4(2) (F1–Au1), 192.4(2) (F2–Au1), 203.5(2) (N1–Au1). Bottom: Molecular structure of [Au-$(N_3)_3$(SIMes)] (**6**) in the solid state. For clarity, only one of the two crystallographically independent molecules in the unit cell is shown (see Figure S4). Thermal ellipsoids are set at 50% probability. Selected bond lengths to the central gold atom [pm]: 202.3(4), *202.3(4)* (C1–Au1), 203.2(4), *203.1(4)* (N1–Au1), 203.1(4), *204.6(4)* (N4–Au1), 203.7(4), *204.3(3)* (N7–Au1). The values in italics denote the bond lengths for the second molecule, which is not shown here.

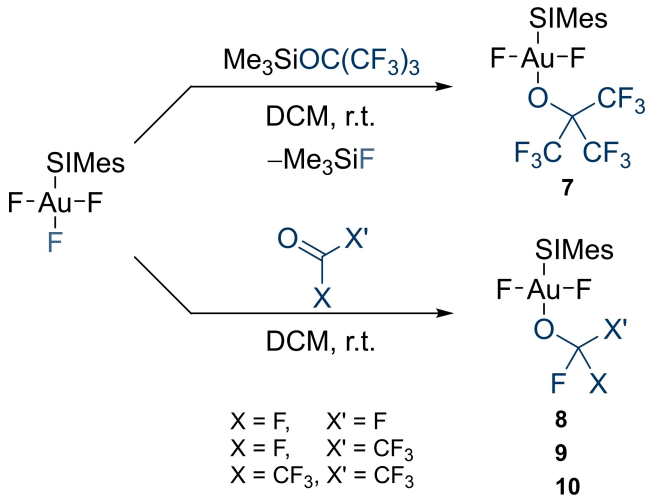

Scheme 4. Reaction of $[AuF_3(SIMes)]$ with $Me_3SiOC(CF_3)_3$ (top) and different perfluorinated carbonyl-bearing molecules (bottom) for the formation of perfluoroalkoxido gold(III) complexes **7**–**10**.

chemical shift of 155.7 ppm, only 3 ppm high-field shifted compared to $[AuF_3(SIMes)]$, indicating a comparable Lewis acidity (see below).

Crystals of *trans*-$[AuF_2(OC(CF_3)_3)(SIMes)]$ (**7**) suitable for X-ray diffraction were obtained by slow vapor diffusion of *n*-pentane onto a concentrated solution of the reaction mixture in DCM at 4 °C. Compound **7** crystallizes in the monoclinic space group $P2_1/n$ with two disordered DCM molecules (see Figure S5), showing the typical square-planar coordination around the gold atom (see Figure 4). The Au–$C_{carbene}$ bond length of 198.4(6) pm is comparable to $[AuF_3(SIMes)]$,[14] indicating the highly Lewis acidic character of the newly formed moiety of **7**.

Turning to the lighter homologues of perfluorinated alkoxides, the corresponding trimethylsilyl compounds are unknown. Inspired by examples of trifluoromethylation reactions using carbonyl fluoride and a fluoride salt,[51,53] we envisioned the investigation of the reactivity of $[AuF_3(SIMes)]$ with carbonyl fluoride and other perfluorinated, carbonyl-bearing molecules, in order to obtain the corresponding alkoxido complexes (Scheme 4, bottom).

Addition of an excess of COF_2 onto a solution of $[AuF_3(SIMes)]$ in DCM leads to the formation of the desired product *trans*-$[AuF_2(OCF_3)(SIMes)]$ (**8**). Its ^{19}F NMR spectrum shows a triplet and a quartet at −40.2 ppm and −314.1 ppm, respectively, with a coupling constant $^4J(^{19}F,^{19}F) = 1.9$ Hz (see Figure 5). The chemical shift of the OCF_3 group is similar to that of the only literature-known trifluoromethoxido gold complex, which is an NHC-stabilized gold(I) complex.[49]

In analogy to the reaction with COF_2, addition of an excess of $CO(CF_3)F$ or $CO(CF_3)_2$ to a solution of $[AuF_3(SIMes)]$ in DCM yields the compounds *trans*-$[AuF_2(OC(CF_3)F_2)(SIMes)]$ (**9**) and *trans*-$[AuF_2(OC(CF_3)_2F)(SIMes)]$ (**10**), respectively, as identified by multinuclear NMR spectroscopy (see Table 1). The ^{19}F NMR spectrum of compound **10** is depicted in Figure 6 and consists of a doublet of triplets at −82.0 ppm, a triplet of septets at −112.0 ppm and a doublet of septets at −313.8 ppm (see Table 1). Due to the high linewidth of the signals and small coupling constants of 1.7 Hz, 2.4 Hz and 3.2 Hz, the complex splitting patterns of the latter two cannot be directly seen in the ^{19}F NMR spectrum but were obtained via simulation (see Figure S47). Similarly, for compound **9**, no $^{19}F,^{19}F$ couplings can be resolved in the ^{19}F NMR spectrum. However, the signals that were assigned to compound **9** (−63.1 ppm, −86.1 ppm and −314.8 ppm, see Table 1) show a cross-peak in the $^{19}F,^{19}F$-COSY NMR spectrum (see Figure S41).

Crystals of compound **10** suitable for X-ray diffraction were obtained by vapor diffusion of *n*-pentane onto a solution of the reaction mixture in DCM. The molecular structure of *trans*-$[AuF_2(OC(CF_3)_2F)(SIMes)]$ (**10**) in the solid state is shown in Figure 6. Compound **10** crystallizes in the triclinic space group $P\bar{1}$. The Au–$C_{carbene}$ and Au–O bond lengths of 197.8(2) pm and 201.3(2) pm, respectively, are comparable to the ones in compound **7** (198.4(6) pm and 202.7(4) pm, respectively, cf. Figure 4). Note, that the structure contains a co-crystallized solvent molecule and a disorder in the heptafluoro-iso-propyl group (see Figure S6).

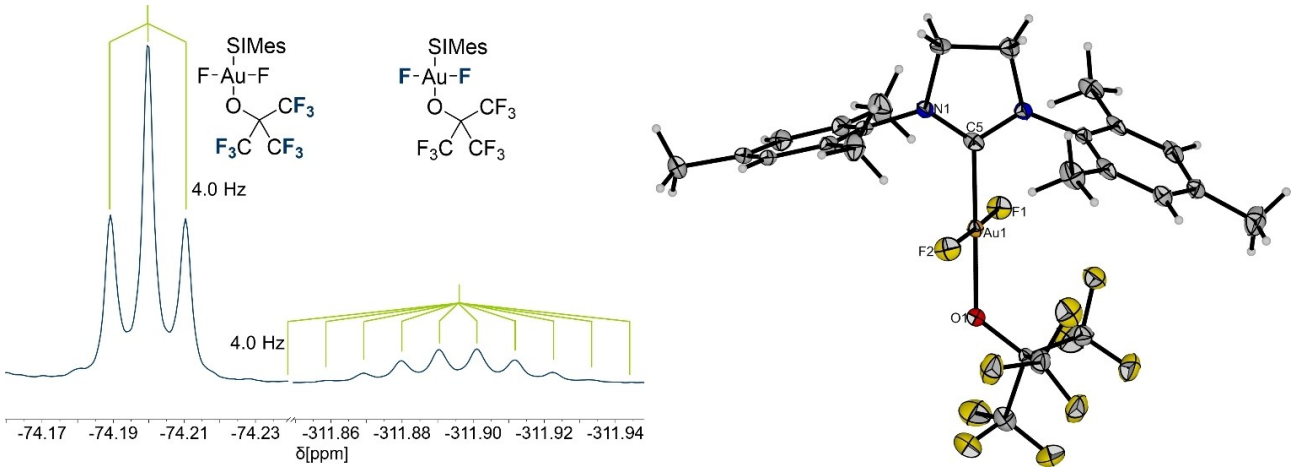

Figure 4. Left: ^{19}F NMR spectrum (377 MHz, DCM-d_2, 18 °C) of *trans*-[$AuF_2(OC(CF_3)_3)(SIMes)$] (**7**). Right: Molecular structure of *trans*-[$AuF_2(OC(CF_3)_3)(SIMes)$]·2 CH_2Cl_2 (**7**·2 CH_2Cl_2) in the solid state. The solvent molecules are omitted for clarity (see Figure S5). Thermal ellipsoids are set at 50% probability. Selected bond lengths to the central gold atom [pm]: 198.4(6) (C5–Au1), 192.5(3) (F1–Au1), 192.1(3) (F2–Au1), 202.7(4) (O1–Au1).

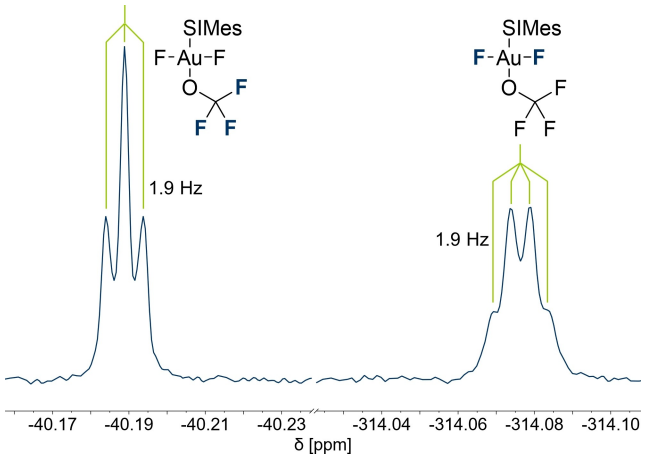

Figure 5. ^{19}F NMR spectrum (377 MHz, DCM-d_2, 18 °C) of *trans*-[$AuF_2(OCF_3)(SIMes)$] (**8**).

Comparing the four perfluoroalkoxido gold complexes **7**–**10**, it can be seen that the stability of the compound increases with the size of the perfluoroalkoxy group. While the trifluoromethoxido (**8**) and the pentafluoroethoxido (**9**) complexes decompose in solution within days (see Figure S36 and Figure S37 for **8**, as well as Figure S42 and Figure S43 for **9**) and have so far escaped crystallization, the heptafluoro-iso-propoxido (**10**) and nonafluoro-*tert*-butoxido (**7**) complexes are far more stable (see Figure S48 and Figure S49 for **10**), which also manifests in the successful crystallization of compounds **7** and **10**. This trend is also underlined by quantum-chemical calculations on the RI-B3LYP-D3/def2-TZVPP level of theory of the reaction energy of [AuF_3(SIMes)] and the corresponding perfluorinated carbonyl-bearing molecules to form compounds **8**–**10**. The Gibbs free energy $\Delta_r G$ for the formation of **8**, **9** and **10** at room temperature is 6 kJ·mol^{-1}, 1 kJ·mol^{-1} and −20 kJ·mol^{-1}, respectively, showing that the formation of the rather unstable compounds **8** and **9** is even slightly endergonic.

After the successful preparation of the perfluoroalkoxido gold complexes, we wanted to investigate the possibility of preparing the non-fluorinated analogues as well. As a test reaction, we tried to use acetone under the same conditions as for the reaction with hexafluoroacetone for the preparation of compound **10**. However, no reaction to the corresponding product *trans*-[$AuF_2(OC(CH_3)_2F)(SIMes)$] was observed, as the corresponding NMR spectra only showed the signals of the starting materials. Another reaction using benzophenone did not yield any new species, either. Therefore, the electrophilicity of the carbon atom in the used carbonyl-bearing molecule seems to play an important role. Furthermore, quantum-chemical calculations show that the Gibbs free energy $\Delta_r G$ at room temperature is 38 kJ·mol^{-1} for the reaction of [AuF_3(SIMes)] with acetone compared to −20 kJ·mol^{-1} for hexafluoroacetone.

SIMes affinity and Au–C bond lengths

As described above, the chemical shift of the carbene carbon atom $\delta(^{13}C_{carbene})$ is highly sensitive to the chemical environment of the SIMes and can be used as a measure of Lewis acidity of the corresponding gold(III) complex. It was shown by our group that this chemical shift correlates with the calculated "SIMes affinity" of those gold(III) moieties at the RI-B3LYP-D3/def2-TZVPP level of theory. The SIMes affinity was defined as the calculated Gibbs free energy $\Delta_r G_{diss}$ of the hypothetical dissociation of an [AuF_2X(SIMes)] or [AuX_3(SIMes)] complex into the free SIMes and the corresponding {AuF_2X} or {AuX_3} fragment, respectively. A nearly linear dependency can be found, i.e. the more upfield-shifted the chemical shift, the higher the SIMes affinity of the respective complex.[16,17] Figure 7 shows an updated version of this correlation including the new compounds **1**–**10**, together with related literature-known complexes.[14,16,17,65,66] All compounds **1**–**10** fit well within the whole set of complexes, underlining that this correlation is valid

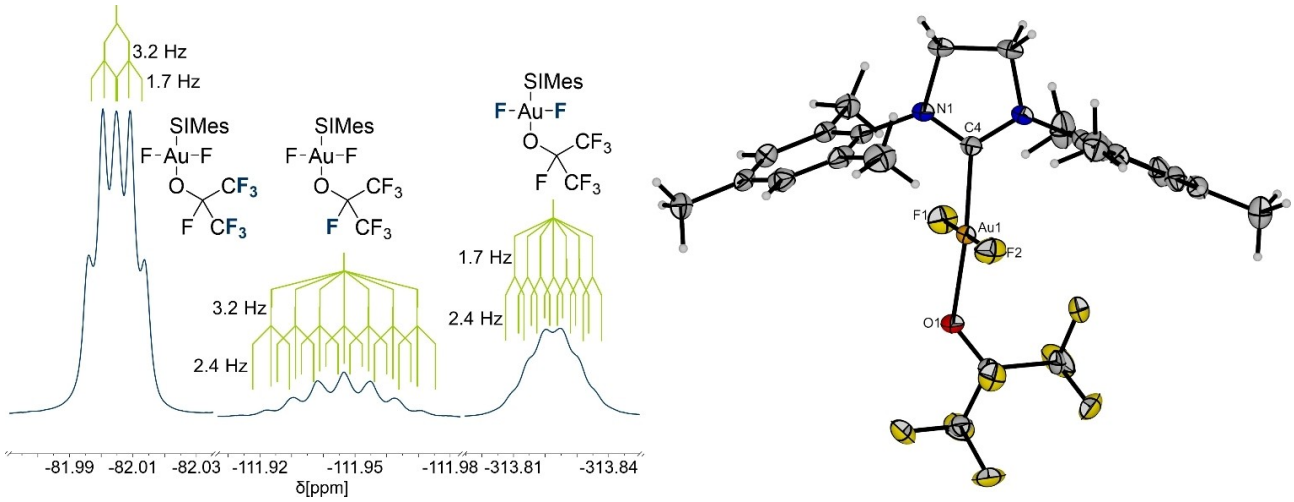

Figure 6. Left: ^{19}F NMR spectrum (377 MHz, DCM-d_2, 16 °C) of *trans*-[$AuF_2(OC(CF_3)_2F)$(SIMes)] (**10**). Right: Molecular structure of *trans*-[$AuF_2(OC(CF_3)_2F)$(SIMes)]·CH_2Cl_2 (**10**·CH_2Cl_2) in the solid state. The disorder in the heptafluoro-*iso*-propyl group and the solvent molecule are omitted for clarity (see Figure S6). Thermal ellipsoids are set at 50% probability. Selected bond lengths to the central gold atom [pm]: 197.8(2) (C4–Au1), 192.3(2) (F1–Au1), 192.2(2) (F2–Au1), 201.3(2) (O1–Au1).

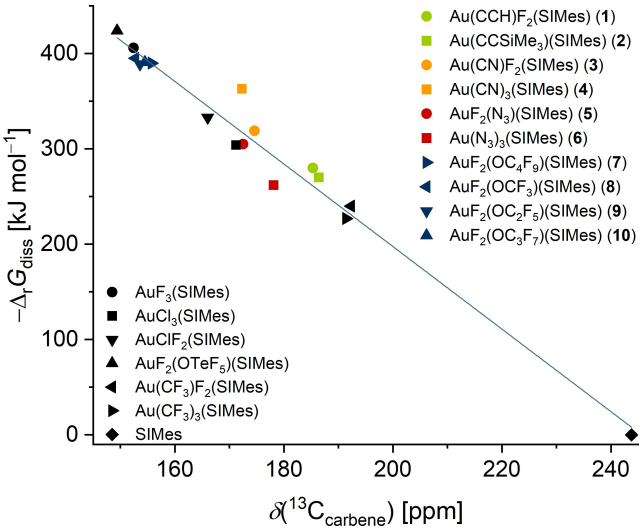

Figure 7. Correlation between the calculated SIMes affinity ($-\Delta_rG_{diss}$) and the chemical shift of the carbene carbon atom in the $^{13}C\{^1H\}$ NMR spectrum ($\delta(^{13}C_{carbene})$) of compounds **1**–**10** (green: alkynido complexes, orange: cyanido complexes, red: azido complexes, blue: perfluoroalkoxido complexes) and related, literature-known compounds (black).[14,16,17,65] The ^{13}C chemical shift of uncoordinated SIMes, which is plotted at a SIMes affinity of 0 kJ·mol^{-1}, is also included.[66]

for a plethora of ligands. Theoretical investigations connected a downfield shift of the carbene carbon atom with the deshielding from a ligand with a strong *trans*-influence.[67] Hence, the ligands can be classified by their *trans*-influence, following the order $OTeF_5 < F < OCF_3 \approx OC_2F_5 \approx OC_3F_7 \approx OC_4F_9 \ll Cl < CN \approx N_3 < CCH \approx CCSiMe_3 < CF_3$. In contrast to a study on gold hydrides, where also the *cis*-influence played a significant role,[68] the ligands in *cis* position do not have a pronounced influence on the deshielding as complexes of the type *trans*-[AuF_2X(SIMes)] and [AuX_3(SIMes)] with identical X have comparable chemical shifts and SIMes affinities.

Furthermore, this correlation can also be extended to the Au–$C_{carbene}$ bond lengths in the solid state. The more electron withdrawing the ligand in *trans* position to the carbene, the more Lewis acidic the gold(III) center and hence, the shorter, i.e. stronger the Au–$C_{carbene}$ bond.[32] This is well reflected in the overview of the Au–$C_{carbene}$ bond lengths of several different *trans*-[AuF_2X(SIMes)] and [AuX_3(SIMes)] complexes (Figure 8),[14,16,17,65] which follows the ordering of the *trans*-influence given above. Furthermore, for the complexes of the type *trans*-[AuF_2X(SIMes)] (X = CCH, CF_3, CN, N_3, OC_3F_7, OC_4F_9, Cl, F, $OTeF_5$), there is also a correlation between the chemical shift of the carbene carbon atom and the Au–C bond lengths (see Figure S50).

Conclusions

In conclusion, a detailed reactivity study of [AuF_3(SIMes)] was performed that gave rise to a variety of products of the type *trans*-[AuF_2X(SIMes)] that were characterized by NMR spectroscopy, structural and computational methods. By using trimethylsilyl compounds, alkynido, cyanido and azido ligands were introduced to the gold center, as well as a perfluoroalkoxido ligand. The pseudohalides cyanide and azide also yielded the corresponding [AuX_3(SIMes)] (X = CN, N_3) complexes when an excess of the Me_3SiX reagent was used. Furthermore, a second pathway, unprecedented in gold chemistry, is described for the introduction of the lighter perfluoroalkoxides consisting of the insertion of the corresponding perfluorinated carbonyl-bearing molecules into the Au–F bond *trans* to the SIMes ligand. Interestingly, the electrophilicity of the carbon atom was found to be crucial for the success of the reaction, as attempts to use the non-fluorinated analogues did not yield the desired products. Comparison of the perfluoroalkoxido gold complexes revealed that the stability of the complex decreases with

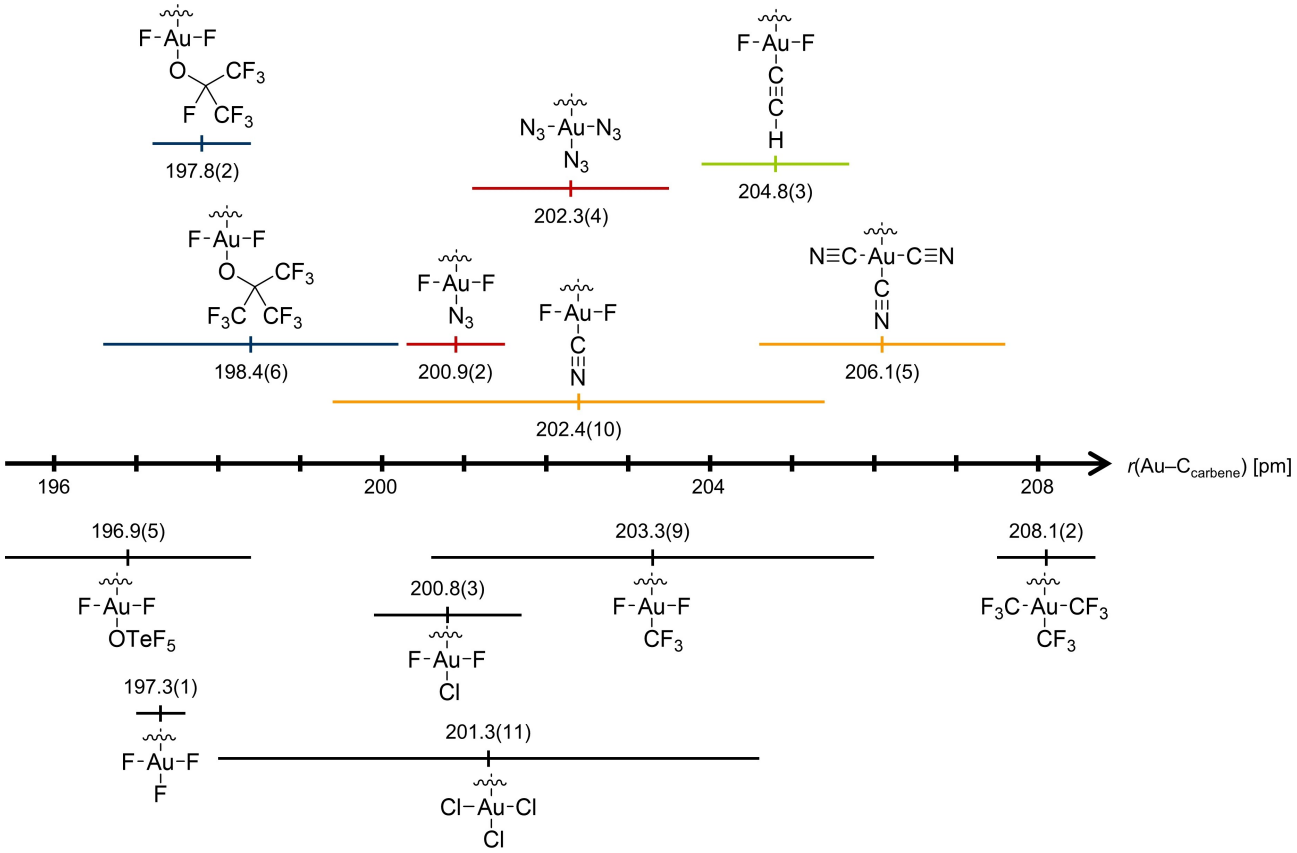

Figure 8. Overview of the Au–C bond lengths r(Au–$C_{carbene}$) of the complexes reported in this paper (top; green: alkynido complexes, orange: cyanido complexes, red: azido complexes, blue: perfluoroalkoxido complexes), and related, literature-known[14,16,17,65] complexes (bottom, black), including a range equal to three times the error in both directions. In the chemical formulae of the structures, the SIMes ligand is omitted for clarity.

smaller perfluorinated moieties bound to the central gold atom, as also supported by quantum-chemical calculations. The ^{13}C NMR chemical shift of the carbene carbon atoms in the prepared compounds was correlated with the calculated SIMes affinity, which, together with similar literature-known complexes, yielded an ordering of more than 10 ligands with respect to their *trans*-influence. The ^{13}C chemical shift was also shown to correlate with the Au–C bond lengths of *trans*-[AuF_2X(SIMes)] complexes. All complexes reported offer several attractive motifs for further reactions such as addition to multiple bonds, or transfer of thermodynamically labile perfluoroalkoxido groups, which could be investigated.

Experimental Section

CAUTION! Strong oxidizers!

All reactions should be conducted under rigorously anhydrous conditions. The presence of organic materials together with AuF_3 can lead to violent reactions. In contact with only small amounts of moisture, all used fluorine-containing substances decompose under the formation of HF. Hence, appropriate treatment procedures need to be available in case of a contamination with HF containing solutions.

Materials, chemicals and procedures: All experiments were performed under strict exclusion of moisture and air using standard Schlenk techniques. Solid compounds were handled inside an *MBRAUN UNIlab plus* glovebox with an argon atmosphere ($c(O_2) <$ 0.5 ppm, $c(H_2O) < 0.5$ ppm). Solvents were dried using an *MBRAUN SPS-800* solvent system and stored over 4 Å molecular sieves. AuF_3,[69] 1,3-bis(2,4,6-trimethylphenyl)-4,5-dihydroimidazol-2-ylidene (SIMes),[70] and [AuF_3(SIMes)][17] were prepared using literature-known syntheses. NMR spectra were recorded with a *JEOL 400 MHz ECZ-R* or *ECS* spectrometer. All chemical shifts are referenced using the Ξ values given in the *IUPAC* recommendations of 2008 and the ^{2}H signal of the deuterated solvent as internal reference.[71] For external locking, acetone-d_6 was flame sealed in a glass capillary and the lock oscillator frequency was adjusted to give $\delta(^1H) =$ 7.26 ppm for a $CHCl_3$ sample locked on the capillary. For spin systems with high linewidths, coupling constants are reported as simulated in *gNMR*.[72] *MestReNova 14.2* was used for processing the spectra and for their graphical representation. X-ray diffraction measurements were performed on a *Bruker D8 Venture* diffractometer with MoK_α ($\lambda = 0.71073$ Å) radiation at 100 K. Single crystals were picked in perfluoroether oil at −40 °C under a nitrogen atmosphere and mounted on a 0.15 mm *Mitegen* micromount. They were solved using the *ShelXT*[73] structure solution program with intrinsic phasing and were refined with the refinement package *ShelXL*[74] using least squares minimizations by using the program *OLEX2*.[75] *Diamond 3* and *POV-Ray 3.7* were used for their graphical representation. Raman spectra of single crystals were recorded at −196 °C using a *Bruker RamanScope III* spectrometer with a resolution of 4 cm^{-1}. The samples were measured using a Teflon plate which is cooled by a copper block cooled with liquid nitrogen,

producing a nitrogen atmosphere that kept the sample inert.[76] IR spectra were measured inside a glovebox under argon atmosphere at room temperature using a *Bruker ALPHA FTIR* spectrometer with a diamond ATR attachment with 32 scans and a resolution of 4 cm^{-1}. Raman and IR spectra were processed using *OPUS 7.5* and *Origin 2022*[77] was used for their graphical representation. Quantum chemical calculations were performed using the functional B3LYP[78] with RI[79] and Grimme-D3[80] corrections and the basis set def2-TZVPP[81] as incorporated in *TURBOMOLE V7.3*.[82] Reaction energies were calculated by subtraction of the energies of the starting materials from the ones of the products, which were obtained from the calculated SCF energy of geometry optimized minimum structures that were corrected for the enthalpy and entropy at standard temperature and pressure using the module *freeh* as incorporated in *TURBOMOLE V7.3* with a scaling factor of 0.9614.[82] All experiments were performed on a 10 mg scale for [AuF_3(SIMes)] and characterized from the reaction mixture.

Reaction between [AuF_3(SIMes)] and Me_3SiCCH: This reaction was performed with varying amounts of Me_3SiCCH and with or without the addition of CsF, see Table S4 for details. In the following, the reaction with CsF and an excess of Me_3SiCCH is described as an example for the procedure, which did not change except for the amounts of substances used. In a typical experiment, [AuF_3(SIMes)] (10 mg, 17.8 μmol, 1 equiv.) and CsF (3 mg, 19,7 μmol, 1.1 equiv.) were dissolved in CD_2Cl_2 (ca. 1 mL) and Me_3SiCCH (18 mg, 188 μmol, 10 equiv.) was condensed onto the frozen solution at −196 °C. The mixture was slowly thawed and the progress of the reaction was followed by NMR spectroscopy. The main reaction product identified by ^{19}F NMR spectroscopy was *trans*-[Au(CCH)F_2(SIMes)] (**1**). However, *trans*-[$AuClF_2$(SIMes)] and traces of *trans*-[Au(CC$SiMe_3$)F_2(SIMes)] (**2**) were formed as side products (see Figure S9–Figure S12). Depending on the amount of Me_3SiCCH and the presence of CsF, the ratio of compound **1** and **2** can vary (cf. Table S4 and Figure S13).

trans-[Au(CCH)F_2(SIMes)] (**1**): **^{1}H NMR** (400 MHz, CD_2Cl_2, 21 °C) δ = 7.07 (s, 4H, *meta*-CH), 4.17 (s, 4H, NCH_2CH_2N), 2.36 (s, 6H, *para*-CH_3), 2.35 (s, 12H, *ortho*-CH_3), 1.60 (t, 1H, −CCH, $^4J(^1H,^{19}F)$ = 2.1 Hz) ppm. **$^{13}C\{^1H\}$ NMR** (101 MHz, CD_2Cl_2, 21 °C) δ = 185.3 (s, NCN carbene), 140.0 (s, C_{Ar}), 136.6 (s, C_{Ar}), 132.2 (s, C_{Ar}), 129.9 (s, C_{Ar}), 51.4 (s, NCH_2CH_2N), 20.9 (s, CH_3), 17.2 (s, CH_3) ppm. **^{19}F NMR** (377 MHz, CD_2Cl_2, 20 °C) δ = −340.8 (d, 2F, *cis*-F, $^4J(^{19}F,^1H)$ = 2.1 Hz) ppm. **IR** $\tilde{\nu}$ = 3305 (w, ν(C-H_{alkyne})), 2924 (w), 2022 (vw, ν(C≡C)), 1607 (w), 1523 (vs), 1459 (s), 1378 (m), 1323 (m), 1273 (vs), 1225 (m), 1185 (m), 1016 (w), 985 (vw), 949 (vw), 924 (vw), 852 (m), 739 (w), 652 (m), 620 (m), 584 (vs, $\nu_{as}(AuF_2)$), 452 (m) cm^{-1}. **FT-Raman** (50 mW, 1024 scans) $\tilde{\nu}$ = 2926 (m), 2031 (m, ν(C≡C)), 1607 (m), 1505 (m), 1384 (m), 1312 (m), 1018 (m), 579 (s, $\nu_{as}(AuF_2)$), 560 (s, $\nu_s(AuF_2)$), 457 (m), 78 (vs) cm^{-1}.

trans-[Au(CC$SiMe_3$)F_2(SIMes)] (**2**): **^{1}H NMR** (400 MHz, CD_2Cl_2, 21 °C) δ = 7.07 (s, 4H, *meta*-CH), 4.15 (s, 4H, NCH_2CH_2N), 2.37 (s, 18H, *ortho*-CH_3 + *para*-CH_3), 0.07 (s, 9H, −CC$SiMe_3$) ppm. **$^{13}C\{^1H\}$ NMR** (101 MHz, CD_2Cl_2, 21 °C) δ = 186.4 (s, NCN carbene), 140.0 (s, C_{Ar}), 136.6 (s, C_{Ar}), 132.0 (s, C_{Ar}), 129.8 (s, C_{Ar}), 51.5 (s, NCH_2CH_2N), 20.6 (s, CH_3), 17.2 (s, CH_3) ppm. **^{19}F NMR** (377 MHz, CD_2Cl_2, 20 °C) δ = −340.2 (s, 2F, *cis*-F) ppm. **$^{29}Si\{^1H\}$-DEPT NMR** (80 MHz, CD_2Cl_2, 21 °C) δ = 7.4 (1Si, −CC$SiMe_3$) ppm.

Reaction between [AuF_3(SIMes)] and $Me_3SiCCSiMe_3$: In a typical experiment, [AuF_3(SIMes)] (10 mg, 17.8 μmol, 1 equiv.), CsF (3 mg, 19,7 μmol, 1.1 equiv.) and $Me_3SiCCSiMe_3$ (6 mg, 35.2 μmol, 2 equiv.) were weighed in and at −196 °C, CD_2Cl_2 (ca. 1 mL) was condensed onto the solids. The mixture was slowly thawed and the progress of the reaction was followed by NMR spectroscopy. The main reaction product identified by ^{19}F NMR spectroscopy was *trans*-[Au(CC$SiMe_3$)F_2(SIMes)] (**2**), whereas *trans*-[$AuClF_2$(SIMes)] is formed as a side product (see Figure S14 and Figure S15).

Reaction between [AuF_3(SIMes)] and Me_3SiCN: In a typical experiment, [AuF_3(SIMes)] (10 mg, 17.8 μmol, 1 equiv.) was dissolved in CD_2Cl_2 (ca. 1 mL) and Me_3SiCN (2 mg, 20.1 μmol, 1.1 equiv.) was condensed onto the frozen solution at −196 °C. The mixture was slowly thawed and the progress of the reaction was followed by NMR spectroscopy. The main reaction product identified by ^{19}F NMR spectroscopy is *trans*-[Au(CN)F_2(SIMes)] (**3**) with some unreacted starting material after one day (see Figure S16–Figure S18). At −196 °C, more Me_3SiCN (5 mg, 54.1 μmol, 3 equiv.) was condensed onto the frozen solution. The progress of the reaction was followed by ^{19}F NMR spectroscopy and a full conversion of [AuF_3(SIMes)] found after one hour, yielding *trans*-[Au(CN)F_2(SIMes)] (**3**) and traces of [Au(CN)$_3$(SIMes)] (**4**), together with an unknown side product. After four weeks, a full conversion of **3** to yield **4** is found (see Figure S19–Figure S21).

trans-[Au(CN)F_2(SIMes)] (**3**): **^{1}H NMR** (400 MHz, CD_2Cl_2, 16 °C) δ = 7.07 (s, 4H, *meta*-CH), 4.23 (s, 4H, NCH_2CH_2N), 2.37 (s, 6H, *para*-CH_3), 2.34 (s, 12H, *ortho*-CH_3) ppm. **$^{13}C\{^1H\}$ NMR** (101 MHz, CD_2Cl_2, 16 °C) δ = 174.6 (s, NCN carbene), 140.5 (s, C_{Ar}), 136.5 (s, C_{Ar}), 131.2 (s, C_{Ar}), 130.0 (s, C_{Ar}), 51.6 (s, NCH_2CH_2N), 21.0 (s, CH_3), 17.1 (s, CH_3) ppm. **^{19}F NMR** (377 MHz, CD_2Cl_2, 16 °C) δ = −337.1 (s, 2F, *cis*-F) ppm. **IR** $\tilde{\nu}$ = 2923 (m), 2161 (w, ν(N≡C)), 1631 (m), 1607 (m), 1533 (vs), 1480 (s), 1460 (s), 1380 (m), 1322 (m), 1276 (vs), 1221 (m), 1187 (m), 1014 (m), 983 (m), 951 (m), 852 (s), 737 (m), 710 (m), 635 (m), 599 (vs, $\nu_{as}(AuF_2)$), 570 (vs, $\nu_s(AuF_2)$), 445 (m), 419 (vs) cm^{-1}.

[Au(CN)$_3$(SIMes)] (**4**): **^{1}H NMR** (400 MHz, CD_2Cl_2, 15 °C) δ = 7.05 (s, 4H, *meta*-CH), 4.29 (s, 4H, NCH_2CH_2N), 2.34 (s, 6H, *para*-CH_3), 2.31 (s, 12H, *ortho*-CH_3) ppm. **$^{13}C\{^1H\}$ NMR** (101 MHz, CD_2Cl_2, 15 °C) δ = 172.3 (s, NCN carbene), 141.1 (s, C_{Ar}), 135.3 (s, C_{Ar}), 130.8 (s, C_{Ar}), 129.6 (s, C_{Ar}), 52.6 (s, NCH_2CH_2N), 20.9 (s, CH_3), 17.7 (s, CH_3) ppm. **IR** $\tilde{\nu}$ = 2920 (w), 2186 (w, ν(N≡C))), 2149 (w, ν(N≡C)), 1607 (m), 1532 (s), 1501 (s), 1457 (s), 1381 (m), 1319 (m), 1275 (vs), 1220 (m), 1188 (m), 1014 (m), 949 (m), 850 (vs), 767 (m), 736 (m), 634 (m), 591 (m), 573 (s), 534 (m), 497 (m), 444 (s), 418 (s) cm^{-1}.

Reaction between [AuF_3(SIMes)] and Me_3SiN_3: In a typical experiment, [AuF_3(SIMes)] (10 mg, 17.8 μmol, 1 equiv.) was dissolved in CD_2Cl_2 (ca. 1 mL) and Me_3SiN_3 (2 mg, 17.4 μmol, 1 equiv.) was condensed onto the frozen solution at −196 °C. The mixture was slowly thawed and the progress of the reaction was followed by NMR spectroscopy. The reaction product identified by ^{19}F NMR spectroscopy is *trans*-[$AuF_2(N_3)$(SIMes)] (**5**) after one hour (see Figure S23–Figure S25). At −196 °C, more Me_3SiN_3 (6 mg, 52.1 μmol, 2.9 equiv.) was condensed onto the frozen solution. The progress of the reaction was followed by ^{19}F NMR spectroscopy and after three days, a full conversion of **5** to yield [Au$(N_3)_3$(SIMes)] (**6**) is found (see Figure S26–Figure S28).

trans-[$AuF_2(N_3)$(SIMes)] (**5**): **^{1}H NMR** (400 MHz, CD_2Cl_2, 16 °C) δ = 7.09 (s, 4H, *meta*-CH), 4.26 (s, 4H, NCH_2CH_2N), 2.37 (s, 6H, *para*-CH_3), 2.36 (s, 12H, *ortho*-CH_3) ppm. **$^{13}C\{^1H\}$ NMR** (101 MHz, CD_2Cl_2, 16 °C) δ = 172.5 (s, NCN carbene), 140.6 (s, C_{Ar}), 136.6 (s, C_{Ar}), 131.7 (s, C_{Ar}), 130.0 (s, C_{Ar}), 51.7 (s, NCH_2CH_2N), 21.0 (s, CH_3), 17.1 (s, CH_3) ppm. **^{19}F NMR** (377 MHz, CD_2Cl_2, 16 °C) δ = −311.1 (s, 2F, *cis*-F) ppm. **IR** $\tilde{\nu}$ = 2923 (m), 2048 (vs, $\nu(N_3)$), 1608 (m), 1534 (vs), 1481 (s), 1463 (s), 1380 (m), 1321 (m), 1277 (vs), 1230 (m), 1191 (m), 1017 (m), 986 (m), 952 (m), 851 (m), 712 (m), 644 (m), 632 (m), 604 (vs, $\nu_{as}(AuF_2)$), 564 (s, $\nu_s(AuF_2)$), 534 (vs), 419 (vs) cm^{-1}.

[Au$(N_3)_3$(SIMes)] (**6**): **^{1}H NMR** (400 MHz, CD_2Cl_2, 15 °C) δ = 7.06 (s, 4H, *meta*-CH), 4.16 (s, 4H, NCH_2CH_2N), 2.42 (s, 12H, *ortho*-CH_3), 2.35 (s, 6H, *para*-CH_3) ppm. **$^{13}C\{^1H\}$ NMR** (101 MHz, CD_2Cl_2, 15 °C) δ = 178.1 (s, NCN carbene), 140.3 (s, C_{Ar}), 136.2 (s, C_{Ar}), 132.0 (s, C_{Ar}), 130.0 (s, C_{Ar}), 51.9 (s, NCH_2CH_2N), 20.9 (s, CH_3), 17.4 (s, CH_3) ppm. **IR**

$\tilde{\nu}$ = 2914 (m), 2039 (vs, $\nu(N_3)$), 2020 (vs, $\nu(N_3)$), 1607 (m), 1523 (s), 1499 (s), 1457 (s), 1376 (m), 1318 (m), 1272 (vs), 1239 (s), 1227 (s), 1183 (m), 1016 (m), 984 (m), 952 (m), 857 (s), 737 (m), 711 (m), 676 (m), 630 (s), 594 (m), 572 (s), 430 (vs), 413 (vs) cm^{-1}. **FT-Raman** (50 mW, 16384 scans) $\tilde{\nu}$ = 2311 (vw), 2239 (vw), 2075 (vw, $\nu(N_3)$), 1580 (vs), 1483 (vs), 1358 (vs), 1086 (vs), 72 (vs) cm^{-1}.

Reaction between [AuF_3(SIMes)] and $Me_3SiOC(CF_3)_3$: In a typical experiment, [AuF_3(SIMes)] (10 mg, 17.8 μmol, 1 equiv.) was dissolved in CD_2Cl_2 (ca. 1 mL) and $Me_3SiOC(CF_3)_3$ (25 mg, 81.1 μmol, 4.5 equiv.) was condensed onto the frozen solution at −196 °C. The mixture was slowly thawed and the progress of the reaction was followed by NMR spectroscopy. The main reaction product identified by ^{19}F NMR spectroscopy was *trans*-[$AuF_2(OC(CF_3)_3)$(SIMes)] (**7**), together with traces of an unknown side product (see Figure S30–Figure S32).

trans-[$AuF_2(OC(CF_3)_3)$(SIMes)] (**7**): **^{1}H NMR** (400 MHz, CD_2Cl_2, 18 °C) δ = 7.08 (s, 4H, *meta*-CH), 4.33 (s, 4H, NCH_2CH_2N), 2.36 (s, 18H, *ortho*-CH_3 + *para*-CH_3) ppm. **^{13}C{^{1}H} NMR** (101 MHz, CD_2Cl_2, 18 °C) δ = 155.7 (s, NCN carbene), 140.6 (s, C_{Ar}), 136.4 (s, C_{Ar}), 131.2 (s, C_{Ar}), 129.8 (s, C_{Ar}), 51.2 (s, NCH_2CH_2N), 20.7 (s, CH_3), 17.1 (s, CH_3) ppm. **^{19}F NMR** (377 MHz, CD_2Cl_2, 18 °C) δ = −74.2 (t, 9F, −OC(CF_3)$_3$, $^5J(^{19}F,^{19}F)$ = 4.0 Hz), −311.9 (dec, 2F, *cis*-F) ppm. **IR** $\tilde{\nu}$ = 2926 (vw), 1701 (vw), 1609 (vw), 1542 (s), 1484 (m), 1380 (w), 1263 (vs, ν(C–C)), 1237 (vs, ν(C–C)), 1168 (vs, ν(C–O)), 1015 (vw), 966 (vs, $\delta_{ip}(CCF_3)$), 855 (m), 725 (s, $\delta_{oop}(CF_3)$), 651 (w), 602 (s, $\nu_{as}(AuF_2)$), 573 (m, ν_s (AuF_2)), 536 (w), 488 (vw), 422 (vw) cm^{-1}. **FT-Raman** (200 mW, 8192 scans) $\tilde{\nu}$ = 2927 (s), 2858 (s), 2083 (vw), 2027 (vw), 1506 (vw), 1313 (vw, ν(C–O)), 573 (s, $\nu_s(AuF_2)$), 537 (vw), 284 (vw), 253 (vw), 72 (vs) cm^{-1}.

Reaction between [AuF_3(SIMes)] and COF_2: In a typical experiment, [AuF_3(SIMes)] (10 mg, 17.8 μmol, 1 equiv.) was dissolved in CD_2Cl_2 (ca. 1 mL) and COF_2 (8 mg, 116 μmol, 6.5 equiv.) was condensed onto the frozen solution at −196 °C. The mixture was slowly thawed and the progress of the reaction was followed by NMR spectroscopy. The main reaction product identified by ^{19}F NMR spectroscopy was *trans*-[$AuF_2(OCF_3)$(SIMes)] (**8**) with traces of unknown side products (see Figure S33–Figure S35). Compound **8** decomposes within four days at room temperature to an unknown side product (see Figure S36 and Figure S37).

trans-[$AuF_2(OCF_3)$(SIMes)] (**8**): **^{1}H NMR** (400 MHz, CD_2Cl_2, 18 °C) δ = 7.09 (s, 4H, *meta*-CH), 4.35 (s, 4H, NCH_2CH_2N), 2.36 (s, 18H, *ortho*-CH_3 + *para*-CH_3) ppm. **^{13}C{^{1}H} NMR** (101 MHz, CD_2Cl_2, 18 °C) δ = 152.7 (s, NCN carbene), 140.9 (s, C_{Ar}), 136.4 (s, C_{Ar}), 131.5 (s, C_{Ar}), 130.0 (s, C_{Ar}), 51.4 (s, NCH_2CH_2N), 20.9 (s, CH_3), 17.1 (s, CH_3) ppm. **^{19}F NMR** (377 MHz, CD_2Cl_2, 18 °C) δ = −40.2 (t, 3F, −OCF_3, $^4J(^{19}F,^{19}F)$ = 1.9 Hz), −314.1 (q, 2F, *cis*-F) ppm.

Reaction between [AuF_3(SIMes)] and $CO(CF_3)F$: In a typical experiment, [AuF_3(SIMes)] (10 mg, 17.8 μmol, 1 equiv.) was dissolved in CD_2Cl_2 (ca. 1 mL) and $CO(CF_3)F$ (13 mg, 116 μmol, 6.5 equiv.) was condensed onto the frozen solution at −196 °C. The mixture was slowly thawed and the progress of the reaction was followed by NMR spectroscopy. The main reaction product identified by ^{19}F NMR spectroscopy was *trans*-[$AuF_2(OC(CF_3)F_2)$(SIMes)] (**9**) with traces of an unknown side product (see Figure S38–Figure S41). Compound **9** decomposes within three days at room temperature to an unknown side product (see Figure S42 and Figure S43).

trans-[$AuF_2(OC(CF_3)F_2)$(SIMes)] (**9**): **^{1}H NMR** (400 MHz, CD_2Cl_2, 17 °C) δ = 7.10 (s, 4H, *meta*-CH), 4.35 (s, 4H, NCH_2CH_2N), 2.36 (s, 18H, *ortho*-CH_3 + *para*-CH_3) ppm. **^{13}C{^{1}H} NMR** (101 MHz, CD_2Cl_2, 17 °C) δ = 153.6 (s, NCN carbene), 140.9 (s, C_{Ar}), 136.5 (s, C_{Ar}), 131.5 (s, C_{Ar}), 130.0 (s, C_{Ar}), 51.5 (s, NCH_2CH_2N), 21.0 (s, CH_3), 17.2 (s, CH_3) ppm. **^{19}F NMR** (377 MHz, CD_2Cl_2, 17 °C) δ = −63.1 (s, 2F, −OCF_2CF_3), −86.1 (s, 3F, −OCF_2CF_3), −314.8 (s, 2F, *cis*-F) ppm.

Reaction between [AuF_3(SIMes)] and $CO(CF_3)_2$: In a typical experiment, [AuF_3(SIMes)] (10 mg, 17.8 μmol, 1 equiv.) was dissolved in CD_2Cl_2 (ca. 1 mL) and $CO(CF_3)_2$ (19 mg, 116 μmol, 6.5 equiv.) was condensed onto the frozen solution at −196 °C. The mixture was slowly thawed and the progress of the reaction was followed by NMR spectroscopy. The main reaction product identified by ^{19}F NMR spectroscopy was *trans*-[$AuF_2(OC(CF_3)_2F)$(SIMes)] (**10**) with traces of an unknown side product (see Figure S44–Figure S47).

trans-[$AuF_2(OC(CF_3)_2F)$(SIMes)] (**10**): **^{1}H NMR** (400 MHz, CD_2Cl_2, 16 °C) δ = 7.09 (s, 4H, *meta*-CH), 4.34 (s, 4H, NCH_2CH_2N), 2.36 (s, 18H, *ortho*-CH_3 + *para*-CH_3) ppm. **^{13}C{^{1}H} NMR** (101 MHz, CD_2Cl_2, 17 °C) δ = 154.5 (s, NCN carbene), 140.9 (s, C_{Ar}), 136.4 (s, C_{Ar}), 130.9 (s, C_{Ar}), 130.0 (s, C_{Ar}), 51.4 (s, NCH_2CH_2N), 20.7 (s, CH_3), 17.1 (s, CH_3) ppm. **^{19}F NMR** (377 MHz, CD_2Cl_2, 16 °C) δ = −82.0 (dt, 6F, −OCF(CF_3)$_2$, $^3J(^{19}F,^{19}F)$ = 3.2 Hz, $^5J(^{19}F,^{19}F)$ = 1.7 Hz), −112.0 (tsept, 1F, −OC*F*(CF_3)$_2$, $^4J(^{19}F,^{19}F)$ ≈ 2.4 Hz), −313.9 (dsept, 2F, *cis*-F) ppm. **FT-Raman** (100 mW, 4096 scans) $\tilde{\nu}$ = 2932 (m), 1609 (w), 1505 (w), 1465 (w), 1390 (w), 1314 (w, ν(C–O)), 1012 (vw), 776 (vw), 567 (m, $\nu_s(AuF_2)$), 422 (vw), 342 (w), 290 (w), 188 (w), 70 (vs) cm^{-1}.

Deposition Numbers 2262531 (for **1**), 2262543 (for **3**), 2262544 (for **4**·CH_2Cl_2), 2262532 (for **5**·0.5 CH_2Cl_2), 2262533 (for **6**), 2262545 (for **7**·2 CH_2Cl_2), 2262534 (for **10**·CH_2Cl_2) contain the supplementary crystallographic data for this paper. These data are provided free of charge by the joint Cambridge Crystallographic Data Centre and Fachinformationszentrum Karlsruhe Access Structures service.

Supporting Information

The authors have cited additional references within the Supporting Information.[14,16,17,83]

Acknowledgements

Funded by the ERC project HighPotOx (Grant agreement ID:818862). The authors would like to thank the HPC Service of ZEDAT, Freie Universität Berlin, for computing time and gratefully acknowledge the assistance of the Core Facility BioSupraMol supported by the DFG. M. W. thanks the Dahlem Research School for financial support, Dr. Günther Thiele for help solving the solid state structures and Elodie Lorentz for help designing the TOC graphic. A. P.-B. and M. A. E. thank the Alexander von Humboldt Foundation for a postdoctoral research fellowship. A. P.-B. also acknowledges the Department of Biology, Chemistry, Pharmacy of the Freie Universität Berlin for a Rising Star Junior Fellowship. Open Access funding enabled and organized by Projekt DEAL.

Conflict of Interests

The authors declare no conflict of interest.

Data Availability Statement

The data that support the findings of this study are available from the corresponding author upon reasonable request.

Keywords: gold(III) · gold fluorides · *N*-heterocyclic carbenes · organo gold chemistry · perfluoroalkoxides

[1] F. Mohr, *Gold Bull.* **2004**, *37*, 164.
[2] D. R. Lide, *CRC Handbook of Chemistry and Physics*, 87. Aufl., Taylor & Francis, Boca Raton, FL., **2006**.
[3] a) W. J. Wolf, F. D. Toste, in *Patai's chemistry of functional groups* (Hrsg.: Z. Rappoport, J. F. Liebman, I. Marek), Wiley, Chichester, **2014**, S. 391–408; b) J. Miró, C. del Pozo, *Chem. Rev.* **2016**, *116*, 11924.
[4] D. S. Laitar, P. Müller, T. G. Gray, J. P. Sadighi, *Organometallics* **2005**, *24*, 4503.
[5] J. A. Akana, K. X. Bhattacharyya, P. Müller, J. P. Sadighi, *J. Am. Chem. Soc.* **2007**, *129*, 7736.
[6] R. Kumar, A. Linden, C. Nevado, *Angew. Chem. Int. Ed.* **2015**, *54*, 14287; *Angew. Chem.* **2015**, *127*, 14495.
[7] a) M. S. Winston, W. J. Wolf, F. D. Toste, *J. Am. Chem. Soc.* **2015**, *137*, 7921; b) R. Kumar, A. Linden, C. Nevado, *J. Am. Chem. Soc.* **2016**, *138*, 13790.
[8] A. Pérez-Bitrián, S. Martínez-Salvador, M. Baya, J. M. Casas, A. Martín, B. Menjón, J. Orduna, *Chem. Eur. J.* **2017**, *23*, 6919.
[9] A. Genoux, J. A. González, E. Merino, C. Nevado, *Angew. Chem. Int. Ed.* **2020**, *59*, 17881; *Angew. Chem.* **2020**, *132*, 18037.
[10] A. Genoux, M. Biedrzycki, E. Merino, E. Rivera-Chao, A. Linden, C. Nevado, *Angew. Chem. Int. Ed.* **2021**, *60*, 4164; *Angew. Chem.* **2021**, *133*, 4210.
[11] a) N. P. Mankad, F. D. Toste, *J. Am. Chem. Soc.* **2010**, *132*, 12859; b) M. Albayer, R. Corbo, J. L. Dutton, *Chem. Commun.* **2018**, *54*, 6832.
[12] A. Pérez-Bitrián, M. Baya, J. M. Casas, A. Martín, B. Menjón, J. Orduna, *Angew. Chem. Int. Ed.* **2018**, *57*, 6517; *Angew. Chem.* **2018**, *130*, 3425.
[13] G. Kleinhans, A. K.-W. Chan, M.-Y. Leung, D. C. Liles, M. A. Fernandes, V. W.-W. Yam, I. Fernández, D. I. Bezuidenhout, *Chem. Eur. J.* **2020**, *26*, 6993.
[14] M. A. Ellwanger, S. Steinhauer, P. Golz, T. Braun, S. Riedel, *Angew. Chem. Int. Ed.* **2018**, *57*, 7210; *Angew. Chem.* **2018**, *130*, 7328–7332.
[15] F. W. B. Einstein, P. R. Rao, J. Trotter, N. Bartlett, *J. Chem. Soc. A* **1967**, 478.
[16] M. A. Ellwanger, C. von Randow, S. Steinhauer, Y. Zhou, A. Wiesner, H. Beckers, T. Braun, S. Riedel, *Chem. Commun.* **2018**, *54*, 9301.
[17] M. Winter, N. Limberg, M. A. Ellwanger, A. Pérez-Bitrián, K. Sonnenberg, S. Steinhauer, S. Riedel, *Chem. Eur. J.* **2020**, *26*, 16089.
[18] L. Sharp-Bucknall, L. Barwise, J. D. Bennetts, M. Albayer, J. L. Dutton, *Organometallics* **2020**, *39*, 3344.
[19] B. Y.-W. Wong, H.-L. Wong, Y.-C. Wong, M.-Y. Chan, V. W.-W. Yam, *Angew. Chem. Int. Ed.* **2017**, *56*, 302; *Angew. Chem.* **2017**, *129*, 308.
[20] V. W.-W. Yam, K. M.-C. Wong, L.-L. Hung, N. Zhu, *Angew. Chem. Int. Ed.* **2005**, *44*, 3107; *Angew. Chem.* **2005**, *117*, 3167.
[21] D. Zhou, W.-P. To, Y. Kwak, Y. Cho, G. Cheng, G. S. M. Tong, C.-M. Che, *Adv. Sci.* **2019**, *6*, 1802297.
[22] B. Y.-W. Wong, H.-L. Wong, Y.-C. Wong, V. K.-M. Au, M.-Y. Chan, V. W.-W. Yam, *Chem. Sci.* **2017**, *8*, 6936.
[23] J. A. Garg, O. Blacque, K. Venkatesan, *Inorg. Chem.* **2011**, *50*, 5430.
[24] V. K.-M. Au, W. H. Lam, W.-T. Wong, V. W.-W. Yam, *Inorg. Chem.* **2012**, *51*, 7537.
[25] V. K.-M. Au, D. P.-K. Tsang, K. M.-C. Wong, M.-Y. Chan, N. Zhu, V. W.-W. Yam, *Inorg. Chem.* **2013**, *52*, 12713.
[26] K. M.-C. Wong, L.-L. Hung, W. H. Lam, N. Zhu, V. W.-W. Yam, *J. Am. Chem. Soc.* **2007**, *129*, 4350.
[27] K. M.-C. Wong, X. Zhu, L.-L. Hung, N. Zhu, V. W.-W. Yam, H.-S. Kwok, *Chem. Commun.* **2005**, 2906.
[28] D. Curran, H. Müller-Bunz, S. I. Bär, R. Schobert, X. Zhu, M. Tacke, *Molecules* **2020**, *25*, 3474.
[29] a) P. Wilkinson, *Gold Bull.* **1986**, *19*, 75; b) I. R. Christie, B. P. Cameron, *Gold Bull.* **1994**, *27*, 12; c) T. A. Green, *Gold Bull.* **2007**, *40*, 105.
[30] E. Bernhardt, M. Finze, H. Willner, *J. Fluorine Chem.* **2004**, *125*, 967.
[31] a) H. G. Raubenheimer, L. Lindeque, S. Cronje, *J. Organomet. Chem.* **1996**, *511*, 177; b) S. Gaillard, A. M. Z. Slawin, S. P. Nolan, *Chem. Commun.* **2010**, *46*, 2742; c) M. A. Celik, C. Dash, V. A. K. Adiraju, A. Das, M. Yousufuddin, G. Frenking, H. V. R. Dias, *Inorg. Chem.* **2013**, *52*, 729; d) J. Ruiz, M. A. Mateo, *Organometallics* **2021**, *40*, 1515.
[32] M. V. Baker, P. J. Barnard, S. K. Brayshaw, J. L. Hickey, B. W. Skelton, A. H. White, *Dalton Trans.* **2005**, 37.
[33] a) D. V. Partyka, J. B. Updegraff, M. Zeller, A. D. Hunter, T. G. Gray, *Organometallics* **2007**, *26*, 183; b) T. J. Del Castillo, S. Sarkar, K. A. Abboud, A. S. Veige, *Dalton Trans.* **2011**, *40*, 8140; c) T. J. Robilotto, N. Deligonul, J. B. Updegraff, T. G. Gray, *Inorg. Chem.* **2013**, *52*, 9659; d) A. R. Powers, I. Ghiviriga, K. A. Abboud, A. S. Veige, *Dalton Trans.* **2015**, *44*, 14747.
[34] T. J. Robilotto, D. S. Alt, H. A. von Recum, T. G. Gray, *Dalton Trans.* **2011**, *40*, 8083.
[35] O. Dada, D. Curran, C. O'Beirne, H. Müller-Bunz, X. Zhu, M. Tacke, *J. Organomet. Chem.* **2017**, *840*, 30.
[36] T. Roth, H. Wadepohl, L. H. Gade, *Eur. J. Inorg. Chem.* **2016**, *2016*, 1184.
[37] E. Schuh, S. Werner, D. Otte, U. Monkowius, F. Mohr, *Organometallics* **2016**, *35*, 3448.
[38] K. Peng, A. Friedrich, U. Schatzschneider, *Chem. Commun.* **2019**, *55*, 8142.
[39] V. Levchenko, S. Øien-Ødegaard, D. Wragg, M. Tilset, *Acta Crystallogr. Sect. E* **2020**, *76*, 1725.
[40] A. Pérez-Bitrián, S. Alvarez, M. Baya, J. Echeverría, A. Martín, J. Orduna, B. Menjón, *Chem. Eur. J.* **2023**, *29*, e202203181.
[41] C. Hansch, A. Leo, R. W. Taft, *Chem. Rev.* **1991**, *91*, 165.
[42] B. Manteau, P. Genix, L. Brelot, J.-P. Vors, S. Pazenok, F. Giornal, C. Leuenberger, F. R. Leroux, *Eur. J. Org. Chem.* **2010**, *2010*, 6043.
[43] C. Hansch, A. Leo, S. H. Unger, K. H. Kim, D. Nikaitani, E. J. Lien, *J. Med. Chem.* **1973**, *16*, 1207.
[44] D. Moujalled, A. R. White, *CNS Drugs* **2016**, *30*, 227.
[45] J. Qiao, Y.-S. Li, R. Zeng, F.-L. Liu, R.-H. Luo, C. Huang, Y.-F. Wang, J. Zhang, B. Quan, C. Shen, X. Mao, X. Liu, W. Sun, W. Yang, X. Ni, K. Wang, L. Xu, Z.-L. Duan, Q.-C. Zou, H.-L. Zhang, W. Qu, Y.-H.-P. Long, M.-H. Li, R.-C. Yang, X. Liu, J. You, Y. Zhou, R. Yao, W.-P. Li, J.-M. Liu, P. Chen, Y. Liu, G.-F. Lin, X. Yang, J. Zou, L. Li, Y. Hu, G.-W. Lu, W.-M. Li, Y.-Q. Wei, Y.-T. Zheng, J. Lei, S. Yang, *Science* **2021**, *371*, 1374.
[46] A. A. Kolomeitsev, M. Vorobyev, H. Gillandt, *Tetrahedron Lett.* **2008**, *49*, 449.
[47] a) R. Koller, K. Stanek, D. Stolz, R. Aardoom, K. Niedermann, A. Togni, *Angew. Chem. Int. Ed. Engl.* **2009**, *48*, 4332; *Angew. Chem.* **2009**, *121*, 4396; b) J.-B. Liu, X.-H. Xu, F.-L. Qing, *Org. Lett.* **2015**, *17*, 5048; c) J.-B. Liu, C. Chen, L. Chu, Z.-H. Chen, X.-H. Xu, F.-L. Qing, *Angew. Chem. Int. Ed.* **2015**, *54*, 11839; *Angew. Chem.* **2015**, *127*, 12005; d) C. Chen, P. Chen, G. Liu, *J. Am. Chem. Soc.* **2015**, *137*, 15648; e) X. Qi, P. Chen, G. Liu, *Angew. Chem. Int. Ed.* **2017**, *56*, 9517; *Angew. Chem.* **2017**, *129*, 9645; f) C. Chen, P. M. Pflüger, P. Chen, G. Liu, *Angew. Chem. Int. Ed.* **2019**, *58*, 2392; *Angew. Chem.* **2019**, *131*, 2414; g) Y.-M. Yang, J.-F. Yao, W. Yan, Z. Luo, Z.-Y. Tang, *Org. Lett.* **2019**, *21*, 8003; h) J. J. Newton, B. J. Jelier, M. Meanwell, R. E. Martin, R. Britton, C. M. Friesen, *Org. Lett.* **2020**, *22*, 1785.
[48] O. Marrec, T. Billard, J.-P. Vors, S. Pazenok, B. R. Langlois, *J. Fluorine Chem.* **2010**, *131*, 200.
[49] C.-P. Zhang, D. A. Vicic, *Organometallics* **2012**, *31*, 7812.
[50] a) T. Besset, P. Jubault, X. Pannecoucke, T. Poisson, *Org. Chem. Front.* **2016**, *3*, 1004; b) A. Tlili, F. Toulgoat, T. Billard, *Angew. Chem. Int. Ed.* **2016**, *55*, 11726; *Angew. Chem.* **2016**, *128*, 11900.
[51] M. E. Redwood, C. J. Willis, *Can. J. Chem.* **1965**, *43*, 1893.
[52] W. B. Farnham, B. E. Smart, W. J. Middleton, J. C. Calabrese, D. A. Dixon, *J. Am. Chem. Soc.* **1985**, *107*, 4565.
[53] M. Nishida, A. Vij, R. L. Kirchmeier, J. M. Shreeve, *Inorg. Chem.* **1995**, *34*, 6085.
[54] G. L. Trainor, *J. Carbohydr. Chem.* **1985**, *4*, 545.
[55] a) A. A. Kolomeitsev, G. Bissky, J. Barten, N. Kalinovich, E. Lork, G.-V. Röschenthaler, *Inorg. Chem.* **2002**, *41*, 6118; b) T. M. Sokolenko, Y. A. Davydova, Y. L. Yagupolskii, *J. Fluorine Chem.* **2012**, *136*, 20; c) B. J. Jelier, J. L. Howell, C. D. Montgomery, D. B. Leznoff, C. M. Friesen, *Angew. Chem. Int. Ed.* **2015**, *54*, 2945; *Angew. Chem.* **2015**, *127*, 2988; d) M.-L. Fu, J.-B. Liu, X.-H. Xu, F.-L. Qing, *J. Org. Chem.* **2017**, *82*, 3702; e) J. W. Lee, D. N. Spiegowski, M.-Y. Ngai, *Chem. Sci.* **2017**, *8*, 6066; f) M. Zhou, C. Ni, Y. Zeng, J. Hu, *J. Am. Chem. Soc.* **2018**, *140*, 6801; g) C.-L. Tong, X.-H. Xu, F.-L. Qing, *Angew. Chem. Int. Ed.* **2021**, *60*, 22915; *Angew. Chem.* **2021**, *133*, 23097.
[56] M. A. Cinellu, G. Minghetti, *Gold Bull.* **2002**, *35*, 11.
[57] S. Komiya, T. Sone, Y. Usui, M. Hirano, A. Fukuoka, *Gold Bull.* **1996**, *29*, 131.
[58] a) B. R. Sutherland, K. Folting, W. E. Streib, D. M. Ho, J. C. Huffman, K. G. Caulton, *J. Am. Chem. Soc.* **1987**, *109*, 3489; b) Y. Usui, M. Hirano, A. Fukuoka, S. Komiya, *Chem. Lett.* **1997**, *26*, 981.
[59] S. Komiya, M. Iwata, T. Sone, A. Fukuoka, *J. Chem. Soc. Chem. Commun.* **1992**, 1109.
[60] Y. Usui, J. Noma, M. Hirano, S. Komiya, *J. Chem. Soc. Dalton Trans.* **1999**, 4397.
[61] Y. Usui, J. Noma, M. Hirano, S. Komiya, *Inorg. Chim. Acta* **2000**, *309*, 151.
[62] W. A. Sheppard, *J. Org. Chem.* **1964**, *29*, 1.

[63] W. A. Herrmann, O. Runte, G. Artus, *J. Organomet. Chem.* **1995**, *501*, C1–C4.
[64] a) D. Schneider, O. Schuster, H. Schmidbaur, *Organometallics* **2005**, *24*, 3547; b) O. Schuster, R.-Y. Liau, A. Schier, H. Schmidbaur, *Inorg. Chim. Acta* **2005**, *358*, 1429.
[65] S. Gaillard, A. M. Z. Slawin, A. T. Bonura, E. D. Stevens, S. P. Nolan, *Organometallics* **2010**, *29*, 394.
[66] A. J. Arduengo III, R. Krafczyk, R. Schmutzler, H. A. Craig, J. R. Goerlich, W. J. Marshall, M. Unverzagt, *Tetrahedron* **1999**, *55*, 14523.
[67] a) J. Vícha, C. Foroutan-Nejad, T. Pawlak, M. L. Munzarová, M. Straka, R. Marek, *J. Chem. Theory Comput.* **2015**, *11*, 1509; b) A. H. Greif, P. Hrobárik, M. Kaupp, *Chem. Eur. J.* **2017**, *23*, 9790.
[68] L. Rocchigiani, J. Fernandez-Cestau, I. Chambrier, P. Hrobárik, M. Bochmann, *J. Am. Chem. Soc.* **2018**, *140*, 8287.
[69] A. G. Sharpe, *J. Chem. Soc.* **1949**, 2901.
[70] a) M. Iglesias, D. J. Beetstra, J. C. Knight, L.-L. Ooi, A. Stasch, S. Coles, L. Male, M. B. Hursthouse, K. J. Cavell, A. Dervisi, I. A. Fallis, *Organometallics* **2008**, *27*, 3279; b) E. L. Kolychev, I. A. Portnyagin, V. V. Shuntikov, V. N. Khrustalev, M. S. Nechaev, *J. Organomet. Chem.* **2009**, *694*, 2454.
[71] R. K. Harris, E. D. Becker, S. M. Cabral de Menezes, P. Granger, R. E. Hoffman, K. W. Zilm, *Pure Appl. Chem.* **2008**, *80*, 59.
[72] Adept Scientific, *gNMR V 5.0*, **2005**.
[73] G. M. Sheldrick, *Acta Crystallogr. Sect. A* **2015**, *71*, 3.
[74] G. M. Sheldrick, *Acta Crystallogr. Sect. C* **2015**, *71*, 3.
[75] O. V. Dolomanov, L. J. Bourhis, R. J. Gildea, J. A. K. Howard, H. Puschmann, *J. Appl. Crystallogr.* **2009**, *42*, 339.
[76] P. Voßnacker, T. Keilhack, N. Schwarze, K. Sonnenberg, K. Seppelt, M. Malischewski, S. Riedel, *Eur. J. Inorg. Chem.* **2021**, *2021*, 1034.
[77] OriginLab Corporation, *OriginPro, Version 2022*, Northampton, MA, USA.
[78] A. D. Becke, *J. Chem. Phys.* **1993**, *98*, 5648.
[79] M. Sierka, A. Hogekamp, R. Ahlrichs, *J. Chem. Phys.* **2003**, *118*, 9136.
[80] S. Grimme, J. Antony, S. Ehrlich, H. Krieg, *J. Chem. Phys.* **2010**, *132*, 154104.
[81] a) F. Weigend, R. Ahlrichs, *Phys. Chem. Chem. Phys.* **2005**, *7*, 3297; b) F. Weigend, M. Häser, H. Patzelt, R. Ahlrichs, *Chem. Phys. Lett.* **1998**, *294*, 143.
[82] TURBOMOLE GmbH, *TURBOMOLE V7.3. a development of University of Karlsruhe and Forschungszentrum Karlsruhe*, **2018**.
[83] E. Schnell, E. G. Rochow, *J. Inorg. Nucl. Chem.* **1958**, *6*, 303.

Manuscript received: May 26, 2023
Accepted manuscript online: June 20, 2023
Version of record online: August 4, 2023